

Integrating roots into a whole plant network of flowering time genes in *Arabidopsis thaliana*

Frédéric Bouché ^{1,2}, Maria D'Aloia ^{1,3}, Pierre Tocquin ¹,
Guillaume Lobet ¹, Nathalie Detry ¹, and Claire Périlleux ^{1*}.

¹ PhytoSYSTEMS, Laboratory of Plant Physiology, University of Liège,
Quartier Vallée 1 Sart Tilman Campus, 4 Chemin de la Vallée, B-4000 Liège, Belgium.

² Current address: Department of Biochemistry, University of Wisconsin-Madison,
433 Babcock Drive, Madison, WI 53706-1544, USA

³ Current address : GlaxoSmithKline Biologicals, Research & Development,
Avenue Fleming 20, 1300 Wavre, Belgium

* For correspondence (Tel: +32 4 3663833, e-mail cperilleux@ulg.ac.be)

Running title:
Rooting the flowering process.

1 ABSTRACT

2 Molecular data concerning the involvement of the roots in the genetic pathways regulating floral
3 transition are lacking. In this study, we performed global analyses of root transcriptome in
4 Arabidopsis in order to identify flowering time genes that are expressed in the roots and genes
5 that are differentially expressed in the roots during the induction of flowering. Data mining of
6 public microarray experiments uncovered that about 200 genes whose mutation was reported to
7 alter flowering time are expressed in the roots but only few flowering integrators were found.
8 Transcriptomic analysis of the roots during synchronized induction of flowering by a single 22-h
9 long day revealed that 595 genes were differentially expressed. A delay in clock gene expression
10 was observed upon extension of the photoperiod. Enrichment analyses of differentially
11 expressed genes in root tissues, gene ontology categories and cis-regulatory elements converged
12 towards sugar signaling. We inferred that roots are integrated in systemic signaling whereby
13 carbon supply coordinates growth at the whole plant level during the induction of flowering.

14

15 INTRODUCTION

16 Flowering is a crucial step of plant development that must be precisely timed to occur when
 17 external conditions are favourable for successful reproduction. Floral induction is therefore
 18 controlled by several environmental and endogenous cues, whose inputs are integrated into
 19 finely-tuned regulatory gene networks. In *Arabidopsis thaliana*, genetic analyses unveiled a
 20 number of flowering pathways that are activated in response to photoperiod, temperature, sugars,
 21 hormones and plant aging, or eventually occurs autonomously (Bouché et al., 2016). These
 22 pathways are not restricted to the shoot apical meristem where flowers are initiated but also
 23 involve the leaves at least, supporting the fact that flowering, as shown previously at the
 24 physiological level, is a systemic process. Clearest evidence came from the photoperiodic
 25 pathway that accelerates flowering in response to increasing daylength to ensure bolting in
 26 spring (Song et al., 2015). A key actor in this pathway is the transcription factor CONSTANS
 27 (CO) whose expression follows a circadian pattern but is degraded in the dark (Suarez-Lopez et
 28 al., 2001; Valverde et al., 2004). Light must therefore coincide with CO synthesis to stabilize the
 29 protein and enable activation of its targets (Valverde et al., 2004). This occurs during long days
 30 in the companion cells of phloem, where CO activates *FLOWERING LOCUS T (FT)* (Samach et
 31 al., 2000). The FT protein then moves systemically (Corbesier et al., 2007) and in the shoot
 32 apical meristem interacts with the transcription factor FD via 14-3-3 proteins (Abe et al., 2005;
 33 Wigge, 2005; Taoka et al., 2011). This flowering activation complex triggers the expression of
 34 genes that are responsible for the conversion of the vegetative shoot apical meristem into an
 35 inflorescence meristem and for the promotion of floral fate in lateral primordia (Ó'Maoiléidigh et
 36 al., 2014).

37 The prominent role of the FT protein in the systemic signaling operating at floral transition
 38 opens questions concerning the role of side molecules that are co-transported from leaf sources
 39 in the phloem and the pleiotropic effects of FT and putative co-transported signals in different
 40 sinks. Sugar loading is the first step of long-distance mass-flow movement in phloem and hence
 41 carbohydrates might influence flowering signals delivery (Dinant and Suarez-Lopez, 2012).
 42 Several reports however indicate that sugars act as flowering signals themselves, at two sites in

the plant. In the leaves, photosynthesis and activity of TREHALOSE-6-PHOSPHATE SYNTHASE 1 (TPS1), which catalyzes the formation of trehalose-6-phosphate (T6P) involved in sugar sensing, are required for the induction of the *FT* gene, even under inductive photoperiod (King et al., 2008; Wahl et al., 2013). The plant so integrates an environmental signal (the activation of *FT* by CO in response to increasing day length) with a physiological signal (the presence of high carbohydrate levels, as indicated by T6P) (Wahl et al., 2013). Interestingly, CO regulates the expression of GRANULE-BOUND STARCH SYNTHASE (GBSS), an enzyme controlling the synthesis of amylose in starch granules, and could thereby mediate modification of transitory starch composition to increase the sugar mobilization at floral transition (Ortiz-Marchena et al., 2014). Using starchless mutant, Corbesier et al. (1998) concluded that starch mobilization was critical for floral induction in conditions which did not involve an increased photosynthetic activity. All those results build evidence for sugar contribution to the florigenic signaling. In the shoot apex, sucrose content increases when *Arabidopsis* plant flowers in response to a photosynthetic long day (King et al., 2008; Corbesier et al., 1998) or eventually in short days (Eriksson et al., 2006). Sugars can induce the expression of flowering genes in the meristem, *e.g.* via the T6P pathway, independently of *FT* (Wahl et al., 2013). Beside sugars, the phloem sap of *Arabidopsis* is also enriched in amino acids and hormones of the cytokinin family when flowering is induced by a photoperiodic change (Corbesier et al., 1998; 2003). Cytokinins can promote flowering by inducing the paralogue of *FT*, *TWIN SISTER OF FT* (*TSF*), in the leaves and downstream flowering genes in the shoot apical meristem (D'Aloia et al., 2011).

If we can infer from the previous section that multiple flowering signals including FT, sugars and hormones are transported in phloem, the signaling route appears as simplified to one way from leaves to the shoot apical meristem. Roots are ignored. At the physiological level though, a shoot-to-root-to-shoot loop has been described to drive sugar and cytokinin fluxes at floral transition in the *Arabidopsis* relative white mustard (Havelange et al., 2000). More directly, tagging of the FT protein with GFP in *Arabidopsis* allowed to detect movement of the fusion protein from overexpressor scion to *ft* mutant rootstock, indicating that it is not restricted to aerial parts of the plant (Corbesier et al., 2007). In other species, FT-like proteins exported from the leaves can induce belowground processes such as tuberization in potato (Navarro et al.,

2011) or bulb formation in onion (Lee et al., 2013). These reports indicate that developmental signals from leaf origin reach the underground organs.

Little information is available about the expression of flowering time genes in the roots. In a few cases only, analysis of expression patterns or phenotyping of mutants included careful examination of the roots and were followed by complementation tests (Bernier and Périlleux, 2005). This rationale was used for *FT*, which is not expressed in the roots but whose partner *FD* is (Abe et al., 2005), raising the possibility of a role for the flowering activation complex in the roots. However, the root-specific expression of *FT* did not rescue the phenotype of *ft* single mutant, indicating that the expression of *FT* in root tissues is not sufficient - albeit it might contribute - to flowering (Abe et al., 2005). Other flowering time mutants such as *fca*, several *squamosa-promoter binding protein like* (*spl3*, *spl9* and *spl10*) or *terminal flower 1* (*tfl1*) show root architecture phenotypes (Macknight et al., 2002; Lachowiec et al., 2015; Yu et al., 2015). Major flowering QTL in *Arabidopsis* were also found to be associated with root xylem secondary growth (Sibout et al., 2008). However, whether those traits indicate root-specific functions or indirect effects of flowering time genes remains to be demonstrated.

The aim of this study was to clarify the role of roots in the flowering process. Two complementary approaches were used. First, data mining of public microarray databases was performed to obtain a global view of flowering-time genes expressed in the roots. Second, the transcriptome of the roots was analysed during the induction of flowering. The set of differential by expressed genes was crossed with publicly available datasets obtained in different contexts for discovering potential regulatory networks.

RESULTS

A majority of flowering-time genes are expressed in roots

Data mining was performed using transcriptomic analyses of roots that are available in the ArrayExpress repository (Kolesnikov et al., 2015) (Figure 1). The whole set of selected experiments contained 1,673 Arabidopsis ATH1 Genome arrays (Supplemental Table 1). For each array, we performed an Affymetrix present/absent call to identify root-expressed genes. Genes were considered as being expressed when transcripts were detected ($p < 0.01$) in at least 50% of the 1,673 arrays. We crossed the results of this filter with a comprehensive list of 306 flowering-time genes that we established in the FLOR-ID database (Bouché et al., 2016). These genes are allocated among different pathways whereby flowering occurs in response to photoperiod, vernalization, aging, ambient temperature, hormones or sugar; an “autonomous pathway” leads to flowering independently of these signals and involves regulators of general processes such as chromatin remodeling, transcriptional machinery or proteasome activity. Eight genes under the control of several converging pathways are defined as “flowering-time integrators”: *FT*, *TSF*, *SUPPRESSOR OF OVEREXPRESSION OF CO1 (SOC1)*, *AGAMOUS-LIKE 24 (AGL24)*, *FRUITFULL (FUL)*, *FLOWERING LOCUS C (FLC)*, *SHORT VEGETATIVE PHASE (SVP)* and *LEAFY (LFY)*. Given the design of ATH1 microarrays, 37 flowering-time genes including 11 genes encoding microRNAs could not be included in our survey because they are not represented in the probe set. Out of the 269 represented flowering time genes, 183 (68%) were expressed in roots in more than half of the analyzed arrays (Figure 1A; Supplemental Table 2). Some flowering pathways were more enriched than others (Figure 1B), e.g. the photoperiodic pathway with 70% of its genes being expressed in the roots or the sugar pathway with 7 genes out of 9 being active in the roots, including *TPS1*. As expected, genes controlling autonomous flowering via general regulatory processes were widely detected in roots (80%). A side category of circadian clock genes was also highlighted in the analysis. By contrast, a low proportion of genes from the hormones and aging pathways could be detected.

120 If we analysed one-by-one the data and focused on master flowering-time genes that are
121 highlighted in flowering snapshots (Bouché et al., 2016), we found that most of them were
122 actually not expressed in the roots or at least did not pass the filter setting of being detected in at
123 least 50% of the available root transcriptomes (Figure 1C). In the photoperiod pathway, *CO* and
124 *FT* were not at all detected in the dataset; only *GIGANTEA* (*GI*) was, which mediates between
125 the clock and *CO* regulation (Mishra and Panigrahi, 2015). The flowering activation complex
126 component FD and its paralogue FDP were not hit on the analysis either (detected in 5% of the
127 arrays only). In the aging pathway, *MIRNA* genes were not analysed on ATH1 arrays, but their
128 *SPL* targets involved in flowering were not found in the majority of root microarrays. In the
129 vernalization pathway, *FLC* was detected in 11% of the arrays only. As could be expected,
130 flower meristem identity genes *LFY* and *APETALA1* (*API*) were not detected at all but the
131 upstream MADS box gene *SOC1* was expressed in 42% of the array.

132 The only pathways whose key regulators are expressed in the roots are the sugar pathway, as
133 *TPS1* was detected in 81% of the arrays, and the ambient temperature pathway, with *SVP* and
134 *FLOWERING LOCUS M* (*FLM*) coming up in 73% and 51% of the arrays analysed,
135 respectively. This finding makes sense since all plant parts undoubtedly sense sugars and
136 surrounding temperature, including the roots.

137 **Root transcriptome changes during the induction of flowering**

138 To identify new candidate genes expressed in the roots and potentially involved in flowering, we
139 analysed root transcriptome during the induction of flowering (Figure 2). Plants were grown in
140 hydroponics for 7 weeks under 8-h short days (8-h SD) and then induced to flower by a single
141 22-h long day (22-h LD), as described in Tocquin et al. (2003). We harvested roots 16 and 22 h
142 after the beginning of the 22-h LD and at the same times in control 8-h SD. We chose these
143 timing points to target early signaling events of floral induction. Two weeks after the
144 experiment, we dissected the remaining intact plants to check that those exposed to the 22-h LD
145 had entered floral transition whereas the 8-h SD controls were still vegetative (Figure 2A). Three
146 independent experiments were performed and used for a transcriptome analysis with Arabidopsis
147 ATH1 genome arrays; the raw results had been included in the data mining reported above. A

total of 10,508 AGI loci passed filtering criteria (see Material and Methods) and thus were considered as being expressed in the roots in our experimental system. These 10,508 loci included 168 flowering-time genes, among which 152 were common with the subset revealed by the global data mining shown in Figure 1, somehow confirming these results. Sixteen additional flowering-time genes were then expressed in our experimental set-up, and hence may be regulated by plant age or growing conditions (Supplemental Table 3). Among them, we found the floral integrator *SOC1* and two flowering-time genes involved in the control of meristem determinacy: *TERMINAL FLOWER 1 (TFL1)*, a gene of the same family as *FT* but repressing floral transition in the shoot apical meristem (Kobayashi et al., 1999) and *XAANTAL2 (XAL2)*, also named *AGL14*, a gene involved in shoot and root development (Garay-Arroyo et al., 2013; Pérez-Ruiz et al., 2015).

The root transcriptome was found to undergo numerous changes during the inductive LD. At h16, *i.e.* 8 hours from the extension of the photoperiod, 86 differentially expressed genes were identified in the roots and at h22, the number had increased to 583 (Figure 2C). We considered genes as being differentially expressed when the adjusted p-value was ≤ 0.01 and fold-change ≥ 2 . The heatmap shows that most changes occurring at h16 were actually amplified at h22 (74 of the 86 differentially expressed genes) (Figure 2B) indicating that the experimental design targeted early events. In total, 595 differentially expressed genes were identified in the roots (Supplemental Table 3) among which 18 known flowering time genes allocated to the photoperiod pathway, the circadian clock and the sugar pathway (Figure 2D). This number thus represented about 10% of all the flowering time genes detected in the roots by data mining.

Members of the photoperiodic pathway included negative regulators of CO: *CYCLING DOF FACTOR2* and 3 (*CDF2/3*), *B-BOX DOMAIN PROTEIN 19 (BBX19)* and *SUPPRESSOR OF PHYA-105 1 (SPA1)* but whereas *CDF2/3* and *BBX19* were down-regulated in LD, *SPA1* was upregulated. Two positive regulators of CO were also up-regulated: *GI* and the blue-light photoreceptor gene *CRYPTOCHROME1 (CRY1)*. Two CO-like genes - *CONSTANS-LIKE5 (COL5)* and *SALT TOLERANCE (STO)* - were down-regulated at h22 in LD, as well as the gene encoding the phytochrome B-interacting protein *VASCULAR PLANT ONE ZINC FINGER PROTEIN 2 (VOZ2)*.

177 Among clock components, several morning genes - *CIRCADIAN CLOCK ASSOCIATED1*
178 (*CCA1*), *LATE ELONGATED HYPOCOTYL (LHY)*, *NIGHT LIGHT-INDUCIBLE AND*
179 *CLOCK-REGULATED2 (LNK2)*, and *REVEILLE2 (RVE2)* - were repressed at h22 in LD. On
180 the opposite, two evening genes were upregulated: *GI* and *EARLY FLOWERING 4 (ELF4)*.

181 The increase in photoperiod also induced the expression of two sugar metabolism-related genes:
182 *TPS1* and *ADP GLUCOSE PYROPHOSPHORYLASE1 (ADG1)*, encoding a subunit of ADP-
183 glucose pyrophosphorylase (AGPase). Finally, we found that the expression of two genes
184 involved in the control of meristem fate was also altered: *TFL1* was upregulated in LD whereas
185 *XAL2* was repressed at h22.

186 **Differentially expressed genes are enriched in phloem tissue**

187 The list of 595 differentially expressed genes was thereafter submitted to different tests to see
188 whether particular networks emerged. We performed three different searches based on (i) tissue
189 enrichment, (ii) gene ontology and (iii) promoter sequences (Figure 3).

190 First, to know in which tissues the differentially expressed genes were enriched, we crossed their
191 list with the tissue-specific root transcriptome dataset published by Brady et al. (2007). As a
192 reference, we used the whole set of 10,508 genes expressed in the roots in our experimental
193 system. We found that while the genes expressed in the roots are mostly detected in xylem and
194 hair cells, this distribution was notably modified in the subset of differentially expressed genes
195 with phloem and lateral root tissues hosting a significant part of the observed changes (Figure
196 3A).

197 Second, we performed a gene ontology enrichment test and found that 'Photoperiodism' was the
198 most significantly enriched term in differentially expressed genes (Figure 3B), followed by
199 'Pyrimidine ribonucleotide biosynthesis', 'Trehalose metabolic processes', 'Response to
200 disaccharide' and 'Circadian rhythm'.

201 Third, we searched for enriched cis-elements in the promoters of differentially expressed genes
202 by using the tools of the MEME suite software (Figure 3C). Differentially expressed genes were

distributed among four subsets corresponding to the expression patterns illustrated in Figure 2B: up or down in LD, at h16 or h22. A *de novo* motif search was then performed with MEME (motif length between 8 and 15 nucleotides) and DREME (motif length ≤ 8) to find the most represented motifs in the promoters of each of the four gene subsets. Based on Korkuc et al. (Korkuc et al., 2014) study, we scanned the regions spanning -500 to +50 nt from the transcription start site of the genes. Among the resulting motifs, we found several close matches to five known cis-elements: the telo-box (AAACCC[TA]), the site II element (A[AG]GCCCCA), the I-Box, the TATCCA element, and the G-box (CACGTG). To determine which of these motifs were specifically associated with the four expression patterns, we tested for the enrichment of each motif in the four subsets of differentially expressed genes with the AME tool. We found that both telo-box and site II elements were significantly enriched in upregulated differentially expressed genes, I-Box and TATCCA were rather associated with repressed differentially expressed genes. The G-box was not significantly enriched in any of the subsets (Figure 3C).

The change in photoperiod affects the root circadian clock

RT-qPCR analyses were performed on selected differentially expressed genes in order to confirm their differential expression (Figure 4). Since several clock genes appeared on the list, we performed time-course experiments to evaluate in more detail to which extent circadian-regulated processes were affected by the photoperiodic treatment. Roots were therefore harvested every 4 h during the inductive 22-h LD and in control 8-h SD.

We analysed the expression of *GI*, *CCA1* and *PSEUDO-RESPONSE REGULATOR 7 (PRR7)* as representative clock genes (Hsu and Harmer, 2014). The 22-h LD caused a 4-h delay in the expression patterns of these three genes, suggesting a phase shift of the circadian clock (Figure 4A, left panel). Since such an effect could globally impact clock outputs, we attempted to evaluate the proportion of clock-regulated genes among the 595 differentially expressed genes. We therefore crossed the list with datasets from transcriptomic analyses of circadian clock-regulated genes in lateral roots (Voß et al., 2015) and shoot (Covington et al., 2008). A large

overlap of 78% and 63% was found with these datasets, respectively, revealing that the majority of the differentially expressed genes were indeed regulated by the circadian clock (Figure 4B).

Our analysis also included candidate genes involved in sugar sensing and cytokinin biosynthesis (Figure 4A, right panel). Most interestingly, *TPSI* whose activity is required for flowering in the leaves and in the shoot apical meristem (Wahl et al., 2013) was up-regulated in the roots during the 22-h LD. Our analysis also showed upregulation in LD of two *ISOPENTENYLTRANSFERASE* encoding genes (*IPT3* and *IPT7*) whereas a third one (*IPT5*) did not vary. These results confirmed the microarray data and clearly suggested that sugar signaling and cytokinin biosynthesis were stimulated in the roots in response to the photoperiodic treatment.

Reverse genetic analysis of differentially expressed genes did not reveal strong phenotypes.

We selected a subset of 30 differentially expressed genes for functional analyses, following a number of criteria such as their expression fold change in the microarray analysis, their root-specific expression pattern (inferred from Covington et al. (2008)'s dataset), their putative function or their novelty (Supplemental Table 4). The corresponding mutants available were characterized for two traits: flowering-time and root architecture (Figure 5). Flowering time was quantified as the total number of leaves below the first flower. Surprisingly, only 5 mutants showed an altered flowering time phenotype in LD (Figure 5A). Some of these mutants had been previously characterized such as *gi-2* which, as expected, was very late flowering (Koornneef et al., 1991) and *glycine-rich RNA-binding protein 7* (*grp7*, also called *ccr2*) which was only slightly delayed (Streitner et al., 2008). The cytokinin biosynthesis mutants *ipt3* and *ipt3;5;7* showed an early flowering phenotype but the latter was highly pleiotropic and displayed abnormal growth (Miyawaki et al., 2006). Finally, the mutant for the *AT3G03870* gene of unknown function showed the earliest flowering phenotype, producing 4 fewer leaves than Col-0 WT.

256 In order to select the genotypes whose root system significantly differed from WT, we performed
 257 a Principal Component Analysis (PCA) using the length of the primary root, the length of the
 258 apical unbranched zone, the lateral root density, the lateral root number, the total lateral root
 259 length and the lateral root angle. The first two Principal Components (PC1 and PC2) were
 260 compared using Student tests with a threshold at $p < 0.01$. The selected genotypes were then
 261 compared to WT for each variable (t-test, $p < 0.01$) (Figure 5B). The first principal component
 262 (PC1), which explained about 45 % of the variability of the dataset, reflects mostly the number of
 263 lateral roots, the length of the primary root, the length of the lateral roots, as well as the length of
 264 the apical unbranched zone of the primary root (Figure 5C). The PC2 mainly reveals lateral root-
 265 related changes, such as their length, their insertion angle on the primary root as well as their
 266 density. The *tps1* mutant was affected in PC1 only, showing reduced length of the apical
 267 unbranched zone as well as shorter primary and lateral roots. The pleiotropic *ipt3;5;7* triple
 268 mutant showed a statistically different PC1, displaying an increased number and density of lateral
 269 roots (Chang et al., 2013). The *ipt3* single mutant also displayed a different PC1, albeit with a
 270 weaker lateral-root phenotype.

271

272 DISCUSSION

273 Molecular data concerning the involvement of the roots in the process of flowering are lacking.
 274 In this study, transcriptome analyses showed that about 200 genes whose mutation had been
 275 shown to alter flowering time are expressed in the roots: 183 were identified in public resources
 276 as being expressed in more than 50% of the arrays and 16 additional genes popped-up in our
 277 experimental design aiming at analysing root transcriptome at floral transition. This data-
 278 crossing relies on an hand-curated database of flowering-time genes that we established recently
 279 (Bouché et al., 2016).

280 The small discrepancy in flowering-time gene numbers found in the two analyses is informative
 281 on the fact that some of these genes might be developmentally regulated in the roots. Indeed,
 282 most arrays deposited in databases were obtained from a few-day old seedlings whereas we
 283 studied mature 7-week old plants. Among the 16 genes expressed in hydroponics but not
 284 reaching the 50% threshold in the data mining survey, we found genes regulating meristem
 285 determinacy in the shoot: *XAL2* and *TFL1*. Most interestingly, *XAL2* is a direct regulator of
 286 *TFL1* expression in the shoot apical meristem but both genes have opposite effects on flowering
 287 time (Shannon and Meeks-Wagner, 1991; Pérez-Ruiz et al., 2015). Both genes also have
 288 opposite effects on root growth: *XAL2* is necessary for normal patterning of root meristem, at
 289 least partly through auxin transport (Garay-Arroyo et al., 2013), whereas *TFL1* was recently
 290 identified as a repressor of root growth (Lachowiec et al., 2015). We observed that the two genes
 291 were differentially expressed in the roots during the 22-h LD, but again in opposite ways: *XAL2*
 292 was down-regulated and *TFL1* was up-regulated, a situation that in the shoot would delay
 293 flowering and in the root would repress growth. The upregulation of *TFL1* in the root is thus
 294 intriguingly similar to what is observed in the shoot meristem where activation of *TFL1* at floral
 295 transition is important to counterbalance incoming flowering signals (Jaeger et al., 2013) but
 296 whether this is relevant in the root requires further investigation.

297 In both the global and experimental microarray analyses, the photoperiodic pathway was found
 298 to be enriched in the roots and several regulators of *CO* were differentially expressed during the
 299 induction of flowering by one LD. Among them we found CDFs and SPA1, involved in the

proteolysis of the CO protein. These results are striking since *CO* itself was not detected in the roots, confirming the very low level reported in other microarray studies (e.g. Birnbaum et al.(2003)). In Takada and Goto (2003), several *CO::GUS* reporter lines showed an expression in the roots while others did not, suggesting that the genomic region in which the transgene is inserted may alter the function of *CO* promoter, which would therefore not reflect its actual expression pattern in roots. Regulators of *CO* thus have other putative targets in the roots, which remain to be discovered. Interestingly, two *CO*-like genes (*COL5* and *STO*) were found to be downregulated during the inductive LD but whether they share regulatory mechanisms with *CO* is currently unknown.

Some genes of the photoperiodic pathway that are expressed in the roots encode photoreceptors, such as *PHYTOCHROME A-B-C*, and *CRYPTOCHROME1-2* (Supplemental Table 2). Direct light effects on root growth are well documented and several reports therefore recommend to conduct experiments with roots kept in darkness (Yokawa et al., 2013; 2014; Silva-Navas et al., 2015). However, numbers of studies on root architecture in *Arabidopsis* are performed *in vitro* and routine protocols consist in growing seedlings in transparent Petri dishes with all parts being illuminated. The majority of the root microarrays used for the data mining were obtained from material harvested in these conditions (1,040 out of 1,673 arrays, Supplemental Table 1). We can then speculate that root illumination introduced a bias in the assembled dataset. By contrast, in our hydroponic device, roots were completely in darkness and hence we can assume that any light effect would be indirect. We tested this hypothesis by crossing our dataset with a transcriptomic analysis of seedling roots grown in the dark and exposed to 1-h red light (Molas et al., 2006). After aligning the filter settings of Molas et al.'s analysis with ours, only 55 genes that were differentially expressed after the 1-h red light treatment were detected in the roots in our hydroponics device. Out of them, 11 were differentially expressed during the 22-h LD, including two flowering-time genes: *STO* and *ELF4* (Supplemental Table 5). It is noteworthy however that if both genes are indeed induced by light and interact with different components of light signaling (Khanna et al., 2003; Indorf et al., 2007), they also exhibit circadian expression pattern (Doyle et al., 2002; Indorf et al., 2007), which is the most likely reason why they were differentially expressed in LD.

330

331 We indeed estimated that around 70% of the genes that are differentially expressed in the roots
 332 during the 22-h LD are regulated by the circadian clock. This proportion is probably
 333 overestimated since it was calculated by crossing our dataset with public databases filtered with
 334 low stringency tools to retrieve rhythmic gene expression patterns (see Materials and Methods).
 335 The clock mechanism was shown in *Arabidopsis* to rely on three interlocking feedback loops
 336 (Hsu and Harmer, 2014). The morning-phased loop comprises *PPR7* and *PPR9* and is activated
 337 by *CCA1* and *LHY*; the evening-loop includes *EARLY FLOWERING 3* (*ELF3*), *ELF4* and
 338 *LUX ARRHYTHMO*, which act together in an evening complex, and other evening genes
 339 including *GI* and *TIMING OF CAB EXPRESSION 1* (*TOC1*). The central loop makes the link
 340 between the two others since *TOC1* activates *CCA1* and *LHY* whereas *CCA1* and *LHY* proteins
 341 repress *TOC1* (Harmer et al., 2000; Alabadi et al., 2001).

342 Interestingly, we found that members of the evening loop - *GI* and *ELF4* - were upregulated
 343 whereas morning genes such as *CCA1* and *LHY* were downregulated in 22-h LD as compared to
 344 8-h SD. These differential expression levels were recorded at the two time points (h16 and h22)
 345 and were probably due to a delay in the expression patterns of these circadian genes upon
 346 extension of the photoperiod, as indicated by the time-course analyses (Figure 5) and also
 347 reported in other studies (de Montaigu et al., 2015). Such changes might reflect the fact that the
 348 circadian clock in plants is entrained to light:dark cycles by photosynthetic inputs. It is known
 349 indeed that sugars derived from photosynthesis entrain the circadian clock through morning genes
 350 in the shoot (Haydon et al., 2013) and that a shoot-derived photosynthesis product is necessary for
 351 the oscillation of the evening genes in the roots (James et al., 2008). Moreover, the circadian
 352 clock orchestrates the coordinate adjustment of carbon partitioning and growth rate that occurs in
 353 response to photoperiod (Yazdanbakhsh et al., 2011). Consistently, we observed the differential
 354 expression of *ADGI*, encoding a subunit of AGPase involved in starch synthesis, and of *TPSI* that
 355 catalyses formation of T6P, during the 22-h LD. T6P was found to mediate the sugar-dependent
 356 post-translational activation of AGPase (Geigenberger, 2011) and hence upregulation of *ADGI*
 357 and of *TPSI* might cooperatively stimulate starch synthesis in the roots during the extension of the
 358 photoperiod. Moreover, T6P was found to be positively correlated with rosette growth rate

(Sulpice et al., 2014) and to be required in the leaves and the shoot apical meristem at flowering (Wahl et al., 2013). All together, our results suggest that roots are integrated in systemic signaling whereby carbon supply coordinates growth at the whole plant level during the induction of flowering. This coordination possibly involves sugar input to the circadian clock and T6P pathway.

This inference is further supported by our *de novo* analysis of the promoters of genes upregulated at h16 and h22 during the 22-h LD. Both time points revealed an enrichment of the telo-box motif, which is present in the promoter of genes expressed in dividing cells of root meristems and is known to mediate the upregulation of glucose-responsive genes (Rook et al., 2006). The telo-box, which would be part of a midnight regulatory module (Michael et al., 2008), is frequently found associated with other motifs, such as the site II element (Trémousaygue et al., 2003; Zografidis et al., 2014) that we also found in our analysis. The functional relevance of the association between these elements has been demonstrated for the SKIP-mediated control of root elongation (Zhang et al., 2012). Conversely, the promoters of genes downregulated during the 22-h LD were found to be enriched in both I-boxes, which are known to be part of a light regulatory module (López-Ochoa et al., 2007), and in the sugar- and gibberellin-responsive element TATCCA, which is bound by MYB factors (Lu et al., 2002). TATCCA element and G-box were also found to be core components of the sugar response sequence (SRS) in the promoter of a sugar starvation-inducible rice α -amylase gene (Amy3, Lu et al. (1998)). These results support a prominent role for sugars in the control of gene expression during the 22-h LD.

Another coincidence is the enrichment of differentially expressed genes in the phloem tissue of the roots, which is the arrival route of sugars transported from the shoot. For example *IPT3* and *IPT7*, two cytokinin-biosynthesis genes expressed in the root vasculature and the endodermis (Hirose et al., 2008), were differentially expressed during the 22-h LD whereas *IPT5*, which is expressed in the root cap, was not. An increased transport of cytokinins from the roots to the aerial part of the plant would establish a feedforward loop promoting flowering since these hormones are known to activate promoters of flowering in the shoot, such as *TSF* in the leaves and *SOCI* in the shoot apical meristem (D'Aloia et al., 2011). These mechanisms provide a

388 molecular basis to the physiological shoot-to-root-to-shoot loop disclosed in the mustard *Sinapis*
389 *alba* where sucrose arriving from the shoot induces cytokinin export from the roots to stimulate
390 floral transition (Havelange et al., 2000).

391 MATERIAL AND METHODS

392 Plant growth

393 All experiments were performed with *Arabidopsis thaliana* Col-0 accession. The *ipt3* single and
394 *ipt3;5;7* triple mutants were provided by Prof. Tatsuo Kakimoto (Osaka University, Japan) and
395 the *gi* mutant was given by Prof. George Coupland (Max Planck Institute for Plant Breeding
396 Research, Köln, Germany). Other mutants were obtained from the Nottingham Arabidopsis
397 Stock Center (<http://www.arabidopsis.info>). Accession numbers are provided in the
398 Supplemental Table 4. All seeds, including Col-0 WT, were bulked at the same time to reduce
399 variability. Plants were grown in hydroponic device made of black containers and accessories
400 (<http://www.araponics.com>). Nutrient solution was a mix of commercial stocks (0.5 ml l⁻¹
401 FloraMicro, FloraGro and FloraBloom; <http://www.generallyhydroponics.com>). Light was
402 provided by fluorescent white tubes at 60 µE.m⁻².s⁻¹ PPFD; temperature was 20°C (day/night)
403 and air relative humidity 70%. For transcriptomic analyses in WT plants, flowering was induced
404 by a single 22-h LD after 7 weeks of growth in 8-h SD and the flowering response was scored as
405 the % of plants having initiated floral buds two weeks after the LD (Tocquin et al., 2003). For
406 mutant phenotyping, plants were cultivated in 16-h LD and duration of vegetative growth was
407 scored as the total number of leaves below the first flower (rosette + cauline leaves) to estimate
408 flowering time.

409 Microarray analysis

410 Roots of 18 individual plants were harvested 16h and 22h after the beginning of the inductive
411 LD and pooled. Sampling at the same times in 8-h SD happened during the dark period and were
412 performed under dim green light. Roots were stored at -80°C until used. Tissues were ground in
413 liquid nitrogen and RNA was extracted with TRizol according to manufacturer's instructions

(www.lifetechnologies.com). Before processing further with the RNA samples, we assessed RNA integrity with the Experiontm automated electrophoresis system (www.bio-rad.com). All the samples used for microarray analysis had maximum RNA quality indicator (RQI) values of 10. The RNA samples were labeled using 3' IVT Expressed kit according to the manufacturer's instructions (Affymetrix, www.affymetrix.com). Three biological replicates obtained from independent experiments were hybridized on ATH1 Genome arrays (Affymetrix). We analyzed raw data using the limma package (Ritchie et al., 2015). Data were GCRMA-normalized and probeset were filtered for an absolute expression level of at least 100 in $\geq 20\%$ of the arrays. We fitted the data to a linear model using the `lmfit()` function, analyzed the variance with the `ebayes()` function, and corrected the p-value for multiple testing using Benjamini and Hochberg's method (Benjamini and Hochberg, 1995). We considered genes as being differentially expressed when the adjusted p-value was ≤ 0.01 and fold-change ≥ 2 .

***In silico* analysis**

Data mining - *In silico* transcriptomic analyses were performed on Arabidopsis Affymetrix ATH1 raw data retrieved from the ArrayExpress database (<http://www.ebi.ac.uk/arrayexpress/>) using the query "roots". The resulting list was manually sorted to remove experiments lacking comprehensive methodological information. Each experiment was manually curated to select only root-specific raw files. The list of experiments included in the survey is available in supplemental material (Supplemental Table 1). The subsequent data analysis was performed using the R programming language (R Core Team). The "simpleaffy" Bioconductor package V.2.44.0 (Huber et al., 2015; Wilson and Miller, 2005) was used to read the raw data and perform the present/absent call on individual arrays using the `detection.p.val()` function. Genes were considered as being expressed when p-value < 0.01 . Within each experiment, we computed the proportion of arrays in which expression of the gene of interest could be detected.

Experimental microarray analyses - The analysis of tissue enrichment was performed using the dataset published in Brady et al. (2007). Each gene represented in the ATH1 arrays was associated with the tissue where its expression level was maximal in Brady's study. The resulting map was used to localize the genes identified in our study and to calculate their

distribution among the different tissues of the roots. This exercise was performed on our microarray analysis with the list of all root-expressed genes (expression level of at least 100 in \geq 20% of the arrays) or the genes differentially expressed during the photoperiodic induction of flowering (adjusted p-value \leq 0.01). Using the resulting data, we performed a Fisher's exact test to determine whether tissues were over- or under-represented in the differentially expressed genes list; the tissues in which the number of differentially expressed genes was higher than the expected value was tested for over-representation while tissues in which the number of differentially expressed genes was lower than the the expect number was tested for under-representation (p-value \leq 0.01).

The Gene Ontology Enrichment analysis was performed using the topGO package V2.20.0 (Alexa and Rahnenfuhrer, 2010) with the annotation of the ATH1 array from ath1121501.db package V3.1.4. We performed a Biological Process (BP) enrichment analysis using the classic Fisher's exact test (p<0.001). Redundant GO terms were removed. The expected numbers of differentially expressed genes were computed based both on the total number of root-expressed genes (see above) and the number of differentially expressed genes in our microarray analysis.

The analysis of circadian clock-regulated genes exploited datasets obtained in studies of the circadian clock in shoots (Covington et al., 2008) and lateral roots (Voß et al., 2015). To identify the shoot circadian clock-regulated genes, Covington and colleagues analyzed different publically available circadian microarray datasets. We used the list containing the highest number of circadian clock-entrained genes. In Voß's study, the authors identified highly-probable circadian clock-regulated genes in the roots using three different analysis tools. The list we selected was based on the less stringent parameters, as we included the genes predicted to be clock-regulated by at least one of those tools. When we crossed our experimental list of differentially expressed genes with these datasets, we found that some differentially expressed genes were not represented in Covington's or Voß's arrays and hence we excluded them for the comparison.

468 RT-qPCR analysis

469 Roots of 18 individual plants were harvested every 4h during the 22-h LD and at the same times
 470 in control 8-h SD. Roots were stored at -80°C until used. Tissues were ground in liquid nitrogen
 471 and RNA was extracted with TRizol according to manufacturer's instructions
 472 (www.lifetechnologies.com). RNA samples were treated with DNase (0.2 U DNase μg^{-1}). We
 473 synthesized first-strand cDNA from 1.5 μg RNA using MMLV reverse transcriptase and
 474 oligo(dT)15 according to manufacturer's instructions (<http://www.promega.com>). Quantitative
 475 PCR (qPCR) reactions were performed in triplicates using SYBR-Green I
 476 (<http://www.eurogentec.com>) in 96-well plates with an iCycler IQ5 (<http://www.bio-rad.com>).
 477 We extracted quantification cycle (Cq) values using the instrument software and imported the data
 478 in qbase^{PLUS} 2.0 (<http://www.biogazelle.com>). A GeNorm analysis (Vandesompele et al., 2002)
 479 was performed in a preliminary experiment to identify suitable reference genes. We selected
 480 *ACTIN2* (*ACT2*) and *TUBULIN2* (*TUB2*) as reference genes for root kinetic expression analysis
 481 (geNorm M value <0.2). The computed geometric mean of their Cq values was used to calculate
 482 the normalization factor, as described in (Vandesompele et al., 2002). The list of primers is
 483 available in Supplemental Table 6.

484 Root phenotyping

485 Plants grown for root architecture analysis were sown in vitro on 0.5x MS supplemented with
 486 1% sucrose. Square Petri dishes were used and placed vertically, under 100 $\mu\text{E.m}^{-2}.\text{s}^{-1}$ PPFD, in
 487 16h-LD. Root pictures were taken every three days using a CCD camera (Canon EOS 1100D
 488 with a Canon Lense EF 50mm 1:1.8) and analyzed using the ImageJ plugin "SmartRoot" (Lobet
 489 et al., 2011). The resulting root tracing were exported and analysed in R (R Core Team). In order
 490 to select the genotypes whose root system significantly differed from WT, we performed a
 491 Principal Component Analysis (PCA) using the length of the primary root, the length of the
 492 apical unbranched zone, the lateral root density, the lateral root number, the total lateral root
 493 length and the lateral root angle. The resulting PC's were compared using Student tests with a
 494 threshold at $p < 0.01$. The selected genotypes were then compared to WT for each variable (t-test,
 495 $p < 0.01$). Data visualization was performed using ggplot2 package (Wickham, 2009).

496 **Cis-elements analysis**

497 For each subsets of similarly controlled genes, we prepared a fasta formatted file containing the
 498 promoter sequences (-500, +50) obtained from the TAIR10 ftp repository (Lamesch et al., 2012).
 499 The analyses were performed using the command line version of the MEME-Suite (Bailey et al.
 500 (2015), <http://meme-suite.org>, version 4.10.0). The parameters for MEME were set as default
 501 values, except for: maximum width of each motif: 15 bp; maximum number of motifs to find:
 502 10; background sequences: all TAIR10 promoters (-500, +50). The parameters for DREME and
 503 AME were set as default values, with the background sequences being the promoters of the
 504 10,508 genes found expressed in roots in this study.

505 **Accession numbers**

506 Microarray data are available in the ArrayExpress database (<http://www.ebi.uk/arrayexpress>)
 507 with the accession numbers E-MTAB-4129 and E-MTAB-4130.

508 **Supplemental data**

509 **Supplemental Table 1:** List of root micro-arrays used for the data-mining analysis.

510 **Supplemental Table 2:** Flowering-time genes in roots.

511 **Supplemental Table 3:** List of genes differentially expressed in the roots during a 22h LD.

512 **Supplemental Table 4:** List of mutants characterized in the present work.

513 **Supplemental Table 5:** List of genes differentially expressed in the roots during a 22h LD and in
 514 Molas et al. (2006).

515 **Supplemental Table 6:** List of primers used for the RT-qPCR analysis

516

517 **ACKNOWLEDGMENTS**

518 The authors would like to thank Kévin Mistiaen for his participation to the setup of microarray
519 analysis pipeline. FB and GL are grateful to the F.R.S.-FNRS for the award of a Ph.D.
520 fellowship (FC 87200) and a postdoctoral research grant (1.B.237.15F) respectively. This
521 research was funded by the Interuniversity Attraction Poles Programme initiated by the Belgian
522 Science Policy Office, P7/29. We thank Prof. Tatsuo Kakimoto (Osaka University, Japan) and
523 Prof. George Coupland (Max Planck Institute for Plant Breeding Research, Köln, Germany) who
524 kindly provided us with *ipt3 / ipt3;5;7* and *gi* seeds, respectively.

525 **AUTHOR CONTRIBUTIONS**

526 FB, MD and CP designed the experiments. FB, MD, and ND performed the experiments. FB did
527 the microarray analysis. PT did the promoter analysis. FB and GL did the data analysis and
528 figures. FB, CP, PT and GL participated to the writing of the manuscript. All co-authors read
529 and approved the final version of the manuscript.

530 **AUTHORS INFORMATIONS**

531 **Frédéric Bouché**, Madison University, fbouche@wisc.edu
532 **Maria D'Aloia**, GlaxoSmithKline Biologicals, maria.x.d-alloia@gsk.com
533 **Pierre Tocquin**, University of Liège, ptoquin@ulg.ac.be
534 **Guillaume Lobet**, University of Liège, guillaume.lobet@ulg.ac.be
535 **Nathalie Detry**, University of Liège, nathalie.detry@ulg.ac.be
536 **Claire Périlleux**, University of Liège, cperilleux@ulg.ac.be

537

538 REFERENCES

- 539 Abe, M., Kobayashi, Y., Yamamoto, S., Daimon, Y., Yamaguchi, A., Ikeda, Y., Ichinoki, H.,
540 Notaguchi, M., Goto, K., and Araki, T. (2005). FD, a bZIP Protein Mediating Signals from
541 the Floral Pathway Integrator FT at the Shoot Apex. *Science* 309: 1052.
- 542 Alabadi, D., Oyama, T., Yanovsky, M.J., Harmon, F.G., Mas, P., and Kay, S.A. (2001).
543 Reciprocal regulation between TOC1 and LHY/CCA1 within the Arabidopsis circadian clock.
544 *Science* 293: 880–883.
- 545 Alexa, A. and Rahnenfuhrer, J. (2010). topGO: enrichment analysis for gene ontology (R package
546 version).
- 547 Bailey, T.L., Johnson, J., Grant, C.E., and Noble, W.S. (2015). The MEME Suite. *Nucleic Acids*
548 *Research* 43: gkv416–W49.
- 549 Benjamini, Y. and Hochberg, Y. (1995). Controlling the False Discovery Rate: A Practical and
550 Powerful Approach to Multiple Testing. *Journal of the Royal Statistical Society. Series B*
551 (Methodological) 57: 289–300.
- 552 Bernier, G. and Périlleux, C. (2005). A physiological overview of the genetics of flowering time
553 control. *Plant Biotechnology Journal* 3: 3–16.
- 554 Birnbaum, K. (2003). A Gene Expression Map of the Arabidopsis Root. *Science* 302: 1956–1960.
- 555 Bouché, F., Lobet, G., Tocquin, P., and Périlleux, C. (2016). FLOR-ID: an interactive database of
556 flowering-time gene networks in Arabidopsis thaliana. *Nucleic Acids Research* 44: D1167–
557 D1171.
- 558 Brady, S.M., Orlando, D.A., Lee, J.Y., Wang, J.Y., Koch, J., Dinneny, J.R., Mace, D., Ohler, U.,
559 and Benfey, P.N. (2007). A High-Resolution Root Spatiotemporal Map Reveals Dominant
560 Expression Patterns. *Science* 318: 801–806.
- 561 Chang, L., Ramireddy, E., and Schmulling, T. (2013). Lateral root formation and growth of
562 Arabidopsis is redundantly regulated by cytokinin metabolism and signalling genes. *Journal*
563 *of Experimental Botany* 64: 5021–5032.
- 564 Corbesier, L., Lejeune, P., and Bernier, G. (1998). The role of carbohydrates in the induction of
565 flowering in Arabidopsis thaliana : comparison between the wild type and a starchless mutant.
566 *Planta* 206: 131–137.
- 567 Corbesier, L., Prinsen, E., Jacqumard, A., Lejeune, P., Van Onckelen, H., Périlleux, C., and
568 bernier, G. (2003). Cytokinin levels in leaves, leaf exudate and shoot apical meristem of
569 Arabidopsis thaliana during floral transition. *Journal of Experimental Botany* 54: 2511–2517.
- 570 Corbesier, L., Vincent, C., Jang, S., Fornara, F., Fan, Q., Searle, I., Giakountis, A., Farrona, S.,

- 571 Gissot, L., Turnbull, C., and Coupland, G. (2007). FT protein movement contributes to long-
572 distance signaling in floral induction of Arabidopsis. *Science* 316: 1030–1033.
- 573 Covington, M.F., Maloof, J.N., Straume, M., Kay, S.A., and Harmer, S.L. (2008). Global
574 transcriptome analysis reveals circadian regulation of key pathways in plant growth and
575 development. *Genome Biology* 9: R130.
- 576 de Montaigu, A., Giakountis, A., Rubin, M., Tóth, R., Cremer, F., Sokolova, V., Porri, A.,
577 Reymond, M., Weinig, C., and Coupland, G. (2015). Natural diversity in daily rhythms of
578 gene expression contributes to phenotypic variation. *Proceedings of the National Academy of*
579 *Sciences of the United States of America* 112: 905–910.
- 580 Dinant, S. and Suarez-Lopez, P. (2012). Multitude of long-distance signal molecules acting via
581 phloem. In *Biocommunication of Plants*, G. Witzany and F. Baluska, eds (*Biocommunication*
582 *of Plants*), pp. 89–121.
- 583 Doyle, M.R., Davis, S.J., Bastow, R.M., McWatters, H.G., Kozma-Bognár, L., Nagy, F., Millar,
584 A.J., and Amasino, R.M. (2002). The ELF4 gene controls circadian rhythms and flowering
585 time in *Arabidopsis thaliana*. *Nature* 419: 74–77.
- 586 D’Aloia, M., Bonhomme, D., Bouché, F., Tamseddak, K., Ormenese, S., Torti, S., Coupland, G.,
587 and Périlleux, C. (2011). Cytokinin promotes flowering of *Arabidopsis* via transcriptional
588 activation of the FT paralogue TSF. *The Plant Journal* 65: 972–979.
- 589 Eriksson, S., Böhlenius, H., Moritz, T., and Nilsson, O. (2006). GA4 is the active gibberellin in
590 the regulation of LEAFY transcription and *Arabidopsis* floral initiation. *Plant Cell* 18: 2172–
591 2181.
- 592 Garay-Arroyo, A., Ortiz-Moreno, E., la Paz Sánchez, de, M., Murphy, A.S., García-Ponce, B.,
593 Marsch-Martínez, N., de Folter, S., Corvera-Poiré, A., Jaimes-Miranda, F., Pacheco-
594 Escobedo, M.A., Dubrovsky, J.G., Pelaz, S., and Alvarez-Buylla, E.R. (2013). The MADS
595 transcription factor XAL2/AGL14 modulates auxin transport during *Arabidopsis* root
596 development by regulating PIN expression. *The EMBO Journal* 32: 2884–2895.
- 597 Geigenberger, P. (2011). Regulation of Starch Biosynthesis in Response to a Fluctuating
598 Environment. *Plant Physiology* 155: 1566–1577.
- 599 Harmer, S.L., Hogenesch, J.B., Straume, M., Chang, H.S., Han, B., Zhu, T., Wang, X., Kreps,
600 J.A., and Kay, S.A. (2000). Orchestrated transcription of key pathways in *Arabidopsis* by the
601 circadian clock. *Science* 290: 2110–2113.
- 602 Havelange, A., Lejeune, P., and bernier, G. (2000). Sucrose/cytokinin interaction in *Sinapis alba*
603 at floral induction: a shoot-to-root-to-shoot physiological loop. *Physiologia Plantarum* 109:
604 343–350.
- 605 Haydon, M.J., Mielczarek, O., Robertson, F.C., Hubbard, K.E., and Webb, A.A.R. (2013).
606 Photosynthetic entrainment of the *Arabidopsis thaliana* circadian clock. *Nature*: 1–15.

- 607 Hirose, N., Takei, K., Kuroha, T., Kamada-Nobusada, T., Hayashi, H., and Sakakibara, H. (2008).
608 Regulation of cytokinin biosynthesis, compartmentalization and translocation. *Journal of*
609 *Experimental Botany* 59: 75–83.
- 610 Hsu, P.Y. and Harmer, S.L. (2014). Wheels within wheels: the plant circadian system. *TRENDS*
611 *in Plant Science* 19: 240–249.
- 612 Huber, W. et al. (2015). Orchestrating high-throughput genomic analysis with Bioconductor.
613 *Nature Methods* 12: 115–121.
- 614 Indorf, M., Cordero, J., Neuhaus, G., and Rodríguez-Franco, M. (2007). Salt tolerance (STO), a
615 stress-related protein, has a major role in light signalling. *The Plant Journal* 51: 563–574.
- 616 Jaeger, K.E., Pullen, N., Lamzin, S., Morris, R.J., and Wigge, P.A. (2013). Interlocking Feedback
617 Loops Govern the Dynamic Behavior of the Floral Transition in Arabidopsis. *The Plant Cell*
618 25: 820–833.
- 619 James, A.B., Monreal, J.A., Nimmo, G.A., Kelly, C.L., Herzyk, P., Jenkins, G.I., and Nimmo,
620 H.G. (2008). The circadian clock in Arabidopsis roots is a simplified slave version of the
621 clock in shoots. *Science* 322: 1832–1835.
- 622 Khanna, R., Kikis, E.A., and Quail, P.H. (2003). EARLY FLOWERING 4 functions in
623 phytochrome B-regulated seedling de-etiolation. *Plant Physiology* 133: 1530–1538.
- 624 King, R.W., Hisamatsu, T., Goldschmidt, E.E., and Blundell, C. (2008). The nature of floral
625 signals in Arabidopsis. I. Photosynthesis and a far-red photoresponse independently regulate
626 flowering by increasing expression of FLOWERING LOCUS T (FT). *Journal of*
627 *Experimental Botany* 59: 3811–3820.
- 628 Kobayashi, Y., Kaya, H., Goto, K., Iwabuchi, M., and Araki, T. (1999). A pair of related genes
629 with antagonistic roles in mediating flowering signals. *Science* 286: 1960–1962.
- 630 Kolesnikov, N., Hastings, E., Keays, M., Melnichuk, O., Tang, Y.A., Williams, E., Dylag, M.,
631 Kurbatova, N., Brandizi, M., Burdett, T., Megy, K., Pilicheva, E., Rustici, G., Tikhonov, A.,
632 Parkinson, H., Petryszak, R., Sarkans, U., and Brazma, A. (2015). ArrayExpress update--
633 simplifying data submissions. *Nucleic Acids Research* 43: D1113–D1116.
- 634 Koornneef, M., Hanhart, C.J., and Veen, J.H. (1991). A genetic and physiological analysis of late
635 flowering mutants in Arabidopsis thaliana. *Molecular & General Genetics* 229: 57–66.
- 636 Korkuc, P., Schippers, J.H.M., and Walther, D. (2014). Characterization and Identification of cis-
637 Regulatory Elements in Arabidopsis Based on Single-Nucleotide Polymorphism Information.
638 *Plant Physiology* 164: 181–200.
- 639 Lachowiec, J., Shen, X., Queitsch, C., and Carlborg, Ö. (2015). A Genome-Wide Association
640 Analysis Reveals Epistatic Cancellation of Additive Genetic Variance for Root Length in
641 Arabidopsis thaliana. *PLoS Genetics* 11: e1005541.

- 642 Lamesch, P., Berardini, T.Z., Li, D., Swarbreck, D., Wilks, C., Sasidharan, R., Muller, R., Dreher,
643 K., Alexander, D.L., Garcia-Hernandez, M., Karthikeyan, A.S., Lee, C.H., Nelson, W.D.,
644 Ploetz, L., Singh, S., Wensel, A., and Huala, E. (2012). The Arabidopsis Information
645 Resource (TAIR): improved gene annotation and new tools. *Nucleic Acids Research* 40:
646 D1202–D1210.
- 647 Lee, R., Baldwin, S., Kenel, F., McCallum, J., and Macknight, R. (2013). FLOWERING LOCUS
648 T genes control onion bulb formation and flowering. *Nature Communications* 4: 1–9.
- 649 Lobet, G., Pagès, L., and Draye, X. (2011). A Novel Image Analysis Toolbox Enabling
650 Quantitative Analysis of Root System Architecture. *Plant Physiology* 157: 29–39.
- 651 López-Ochoa, L., Acevedo-Hernández, G., Martínez-Hernández, A., Argüello-Astorga, G., and
652 Herrera-Estrella, L. (2007). Structural relationships between diverse cis-acting elements are
653 critical for the functional properties of a *rbcS* minimal light regulatory unit. *Journal of*
654 *Experimental Botany* 58: 4397–4406.
- 655 Lu, C.-A., Ho, T.-H.D., Ho, S.-L., and Yu, S.-M. (2002). Three novel MYB proteins with one
656 DNA binding repeat mediate sugar and hormone regulation of alpha-amylase gene
657 expression. *Plant Cell* 14: 1963–1980.
- 658 Lu, C.A., Lim, E.K., and Yu, S.M. (1998). Sugar response sequence in the promoter of a rice
659 alpha-amylase gene serves as a transcriptional enhancer. *Journal of Biological Chemistry* 273:
660 10120–10131.
- 661 Macknight, R., Duroux, M., Laurie, R., Dijkwel, P., Simpson, G., and Dean, C. (2002). Functional
662 significance of the alternative transcript processing of the Arabidopsis floral promoter FCA.
663 *Plant Cell* 14: 877–888.
- 664 Michael, T.P., Mockler, T.C., Breton, G., McEntee, C., Byer, A., Trout, J.D., Hazen, S.P., Shen,
665 R., Priest, H.D., Sullivan, C.M., Givan, S.A., Yanovsky, M., Hong, F., Kay, S.A., and Chory,
666 J. (2008). Network discovery pipeline elucidates conserved time-of-day-specific cis-
667 regulatory modules. *PLoS Genetics* 4: e14.
- 668 Mishra, P. and Panigrahi, K.C. (2015). GIGANTEA – an emerging story. *Frontiers in Plant*
669 *Science* 6: 1–15.
- 670 Miyawaki, K., Tarkowski, P., Matsumoto-Kitano, M., Kato, T., Sato, S., Tarkowska, D., Tabata,
671 S., Sandberg, G., and Kakimoto, T. (2006). Roles of Arabidopsis ATP/ADP
672 isopentenyltransferases and tRNA isopentenyltransferases in cytokinin biosynthesis.
673 *Proceedings of the National Academy of Sciences of the United States of America* 103:
674 16598–16603.
- 675 Molas, M.L., Kiss, J.Z., and Correll, M.J. (2006). Gene profiling of the red light signalling
676 pathways in roots. *Journal of Experimental Botany* 57: 3217–3229.
- 677 Navarro, C., Abelenda, J.A., Cruz-Oró, E., Cuéllar, C.A., Tamaki, S., Silva, J., Shimamoto, K.,
678 and Prat, S. (2011). Control of flowering and storage organ formation in potato by

- 679 FLOWERING LOCUS T. *Nature* 478: 119–122.
- 680 Ortiz-Marchena, M.I., Albi, T., Lucas-Reina, E., Said, F.E., Romero-Campero, F.J., Cano, B.,
681 Ruiz, M.T., Romero, J.M., and Valverde, F. (2014). Photoperiodic Control of Carbon
682 Distribution during the Floral Transition in Arabidopsis. *The Plant Cell* 26: 565–584.
- 683 Ó'Maoiléidigh, D.S., Graciet, E., and Wellmer, F. (2014). Gene networks controlling Arabidopsis
684 thaliana flower development. *The New Phytologist* 201: 16–30.
- 685 Pérez-Ruiz, R.V., García-Ponce, B., Marsch-Martínez, N., Ugartechea-Chirino, Y., Villajuana-
686 Bonequi, M., de Folter, S., Azpeitia, E., Dávila-Velderrain, J., Cruz-Sánchez, D., Garay-
687 Arroyo, A., Sánchez, M. de L.P., Estévez-Palmas, J.M., and Alvarez-Buylla, E.R. (2015).
688 XAANTAL2 (AGL14) Is an Important Component of the Complex Gene Regulatory
689 Network that Underlies Arabidopsis Shoot Apical Meristem Transitions. *Molecular Plant* 8:
690 796–813.
- 691 R Core Team R: A Language and Environment for Statistical Computing (R Foundation for
692 Statistical Computing: Vienna, Austria).
- 693 Ritchie, M.E., Phipson, B., Wu, D., Hu, Y., Law, C.W., Shi, W., and Smyth, G.K. (2015). *limma*
694 powers differential expression analyses for RNA-sequencing and microarray studies. *Nucleic
695 Acids Research* 43: e47–e47.
- 696 Rook, F., Hadingham, S.A., Li, Y., and Bevan, M.W. (2006). Sugar and ABA response pathways
697 and the control of gene expression. *Plant, Cell and Environment* 29: 426–434.
- 698 Samach, A., Onouchi, H., Gold, S.E., Ditta, G.S., Schwarz-Sommer, Z., Yanofsky, M.F., and
699 Coupland, G. (2000). Distinct roles of CONSTANS target genes in reproductive development
700 of Arabidopsis. *Science* 288: 1613–1616.
- 701 Shannon, S. and Meeks-Wagner, D.R. (1991). A Mutation in the Arabidopsis TFL1 Gene Affects
702 Inflorescence Meristem Development. *Plant Cell* 3: 877–892.
- 703 Sibout, R., Plantegenet, S., and Hardtke, C.S. (2008). Flowering as a Condition for Xylem
704 Expansion in Arabidopsis Hypocotyl and Root. *Current Biology* 18: 458–463.
- 705 Silva-Navas, J., Moreno-Risueno, M.A., Manzano, C., Pallero-Baena, M., Navarro-Neila, S.,
706 Téllez-Robledo, B., Garcia-Mina, J.M., Baigorri, R., Javier Gallego, F., and Del Pozo, J.C.
707 (2015). D-Root: a system to cultivate plants with the root in darkness or under different light
708 conditions.: n/a–n/a.
- 709 Song, Y.H., Shim, J.S., Kinmonth-Schultz, H.A., and Imaizumi, T. (2015). Photoperiodic
710 flowering: time measurement mechanisms in leaves. *Annual Review of Plant Biology* 66:
711 441–464.
- 712 Streitner, C., Danisman, S., Wehrle, F., Schöning, J.C., Alfano, J.R., and Staiger, D. (2008). The
713 small glycine-rich RNA binding protein AtGRP7 promotes floral transition in Arabidopsis
714 thaliana. *The Plant Journal* 56: 239–250.

- 715 Suarez-Lopez, P., Wheatley, K., Robson, F., Onouchi, H., Valverde, F., and Coupland, G. (2001).
716 CONSTANS mediates between the circadian clock and the control of flowering in
717 Arabidopsis. *Nature* 410: 1116–1120.
- 718 Sulpice, R., Flis, A., Ivakov, A.A., Apelt, F., Krohn, N., Encke, B., Abel, C., Feil, R., Lunn, J.E.,
719 and Stitt, M. (2014). Arabidopsis coordinates the diurnal regulation of carbon allocation and
720 growth across a wide range of photoperiods. *Molecular Plant* 7: 137–155.
- 721 Takada, S. and Goto, K. (2003). Terminal flower2, an Arabidopsis homolog of heterochromatin
722 protein1, counteracts the activation of flowering locus T by constans in the vascular tissues of
723 leaves to regulate flowering time. *Plant Cell* 15: 2856–2865.
- 724 Taoka, K.-I., Ohki, I., Tsuji, H., Furuita, K., Hayashi, K., Yanase, T., Yamaguchi, M., Nakashima,
725 C., Purwestri, Y.A., Tamaki, S., Ogaki, Y., Shimada, C., Nakagawa, A., Kojima, C., and
726 Shimamoto, K. (2011). 14-3-3 proteins act as intracellular receptors for rice Hd3a florigen.
727 *Nature* 476: 332–335.
- 728 Tocquin, P., Corbesier, L., Havelange, A., Pieltain, A., Kurtem, E., Bernier, G., and Périlleux, C.
729 (2003). A novel high efficiency, low maintenance, hydroponic system for synchronous
730 growth and flowering of Arabidopsis thaliana. *BMC Plant Biology* 3: 1–10.
- 731 Trémousaygue, D., Garnier, L., Bardet, C., Dabos, P., Hervé, C., and Lescure, B. (2003). Internal
732 telomeric repeats and “TCP domain” protein-binding sites co-operate to regulate gene
733 expression in Arabidopsis thaliana cycling cells. *The Plant Journal* 33: 957–966.
- 734 Valverde, F., Mouradov, A., Soppe, W., Ravenscroft, D., Samach, A., and Coupland, G. (2004).
735 Photoreceptor Regulation of CONSTANS Protein in Photoperiodic Flowering. *Science* 303:
736 1003–1006.
- 737 Vandesompele, J., De Preter, K., Pattyn, F., Poppe, B., Van Roy, N., De Paepe, A., and Speleman,
738 F. (2002). Accurate normalization of real-time quantitative RT-PCR data by geometric
739 averaging of multiple internal control genes. *Genome Biology* 3: research0034.1–0034.11.
- 740 Voß, U., Wilson, M.H., Kenobi, K., Gould, P.D., Robertson, F.C., Peer, W.A., Lucas, M.,
741 Swarup, K., Casimiro, I., Holman, T.J., Wells, D.M., Péret, B., Goh, T., Fukaki, H.,
742 Hodgman, T.C., Laplace, L., Halliday, K.J., Ljung, K., Murphy, A.S., Hall, A.J., Webb,
743 A.A.R., and Bennett, M.J. (2015). The circadian clock rephases during lateral root organ
744 initiation in Arabidopsis thaliana. *Nature Communications* 6: 7641.
- 745 Wahl, V., Ponnu, J., Schlereth, A., Arrivault, S., Langenecker, T., Franke, A., Feil, R., Lunn, J.E.,
746 Stitt, M., and Schmid, M. (2013). Regulation of Flowering by Trehalose-6-Phosphate
747 Signaling in Arabidopsis thaliana. *Science* 339: 704–707.
- 748 Wickham, H. (2009). ggplot2 (Springer New York: New York, NY).
- 749 Wigge, P.A. (2005). Integration of Spatial and Temporal Information During Floral Induction in
750 Arabidopsis. *Science* 309: 1056–1059.

751 Wilson, C.L. and Miller, C.J. (2005). Simpleaffy: a BioConductor package for Affymetrix Quality
752 Control and data analysis. *Bioinformatics* 21: 3683–3685.

753 Yazdanbakhsh, N., Sulpice, R., Graf, A., Stitt, M., and Fisahn, J. (2011). Circadian control of root
754 elongation and C partitioning in *Arabidopsis thaliana*. *Plant, Cell and Environment* 34: 877–
755 894.

756 Yokawa, K., Fasano, R., Kagenishi, T., and Baluska, F. (2014). Light as stress factor to plant
757 roots - case of root halotropism. *Frontiers in Plant Science* 5: 718.

758 Yokawa, K., Kagenishi, T., and Baluska, F. (2013). Root photomorphogenesis in laboratory-
759 maintained *Arabidopsis* seedlings. *TRENDS in Plant Science* 18: 117–119.

760 Yu, N., Niu, Q.-W., Ng, K.-H., and Chua, N.-H. (2015). The Role of miR156/SPLs Modules in
761 *Arabidopsis* Lateral Root Development. *The Plant Journal* 83: 673–685.

762 Zhang, X., Ju, H.-W., Huang, P., Chung, J.-S., and Kim, C.S. (2012). Functional identification of
763 AtSKIP as a regulator of the cell cycle signaling pathway in *Arabidopsis thaliana*. *Journal of*
764 *Plant Biology* 55: 481–488.

765 Zografidis, A., Kapolas, G., Podia, V., Beri, D., Papadopoulou, K., Milioni, D., and Haralampidis,
766 K. (2014). Transcriptional regulation and functional involvement of the *Arabidopsis*
767 *pescadillo* ortholog AtPES in root development. *Plant Science* 229: 53–65.

768

769

770 FIGURES LEGENDS

771 **Figure 1. Flowering-time genes expressed in the roots of *Arabidopsis*** 772 ***thaliana*.**

773 Root-expressed genes were identified by a present/absent call on 1,673 root ATH1 arrays
774 retrieved from ArrayExpress repository (<https://www.ebi.ac.uk/arrayexpress/>). Flowering-time
775 genes were extracted from FLOR-ID. **A.** All 306 flowering genes. **B.** Pie charts showing the
776 same set of genes classified into flowering time pathways, circadian clock and flower
777 development. Some genes are involved in more than one pathway. Pie chart area is proportional
778 to gene number. **C.** The snapshot of flowering pathways was extracted and adapted from FLOR-
779 ID. Genes highlighted in green boxes were detected in $\geq 50\%$ of root arrays. Genes in blue boxes
780 were detected in $< 50\%$ arrays. Genes and compounds not analyzed in ATH1 arrays are in grey.

781 **Figure 2. Root transcriptome changes during the induction of** 782 **flowering by a single 22-h LD.**

783 **A.** Experimental design. The proportions of plants having initiated flower buds two weeks after
784 the experiment are shown on the right. **B.** Heatmap of the differentially expressed genes
785 (adjusted p-value ≤ 0.01 ; fold-change ≥ 2) showing three independent biological replicates per
786 condition. Low expression levels in red, high expression levels in green. Relative expression
787 values are scaled per transcript (lines). **C.** Venn diagram of differentially expressed genes at both
788 sampling time points. **D.** List of differentially expressed flowering-time genes.

789

790 **Figure 3. Enrichment analyses of the 595 genes differentially**
 791 **expressed in the roots during an inductive 22-h LD.**

792 **A.** Tissue enrichment. For each gene, expression was localized in the tissue where Brady et al.
 793 (2007) found highest transcript level. In each tissue, the number of differentially expressed genes
 794 is indicated in bold whereas the number of genes that would be expected for this dataset is
 795 enclosed within brackets. Shaded area shows p-values > 0.01. Over- and under-represented
 796 genes are separated by the horizontal dashed red line. **B.** Gene ontology term enrichment in the
 797 list of 595 differentially expressed genes. The number of differentially expressed genes
 798 experimentally associated with each term is indicated in bold, whereas the number of genes
 799 associated with the GO term that would be expected by chance for this dataset is enclosed within
 800 brackets. Bars indicate the $-\log_{10}(\text{p-value})$ for each term (Fisher's exact test). **C.** Motif
 801 enrichment analysis in the -500 to +50 nt region of the genes that were down- or up-regulated at
 802 h16 or at h22 in LD. Numbers are the p-values of motifs that were identified as enriched by
 803 AME at $p < 0.05$ in any of the 4 differentially expressed gene subsets. / indicates non-enriched
 804 motif.

805 **Figure 4. Temporal aspects of transcriptomic changes.**

806 **A.** Time-course analyses of candidate gene expression. Relative transcript levels were analysed
 807 by RT-qPCR during an 8-h SD (closed symbols) or a single 22-h LD (open symbols). Boxes in
 808 the bottom show light (white) and dark (black) periods. Data were normalized using *ACT2* and
 809 *UBQ10* genes. Error bars indicate the standard error of the mean for three experimental
 810 replicates. Data are from one representative experiment. **B.** Estimate of circadian clock-regulated
 811 differentially expressed genes. Venn diagrams showing the overlap between the differentially
 812 expressed genes identified in this study and the circadian clock-regulated genes expressed in
 813 lateral roots [left; Dataset from Voß et al. (2015)] or in the shoot [right; Dataset from Covington
 814 et al. (2008)].

815

816 **Figure 5. Flowering-time and root architecture phenotypes of selected**
817 **mutants in 16-h LD.**

818 **A.** Total number of leaves below the first flower (n=15). * indicates a significant difference with
819 WT Col-0 (Tukey's HSD test, $p < 0.05$). *** indicates a highly significant difference with WT
820 (Tukey's HSD test, $p < 0.01$). WT is shown in blue. **B.** Plot of the first two components of the
821 Principal Component Analysis performed on root system architecture features. **C.** Biplot of the
822 two first components of the PCA. Orange color indicates significant differences with the WT
823 Col-0.

824

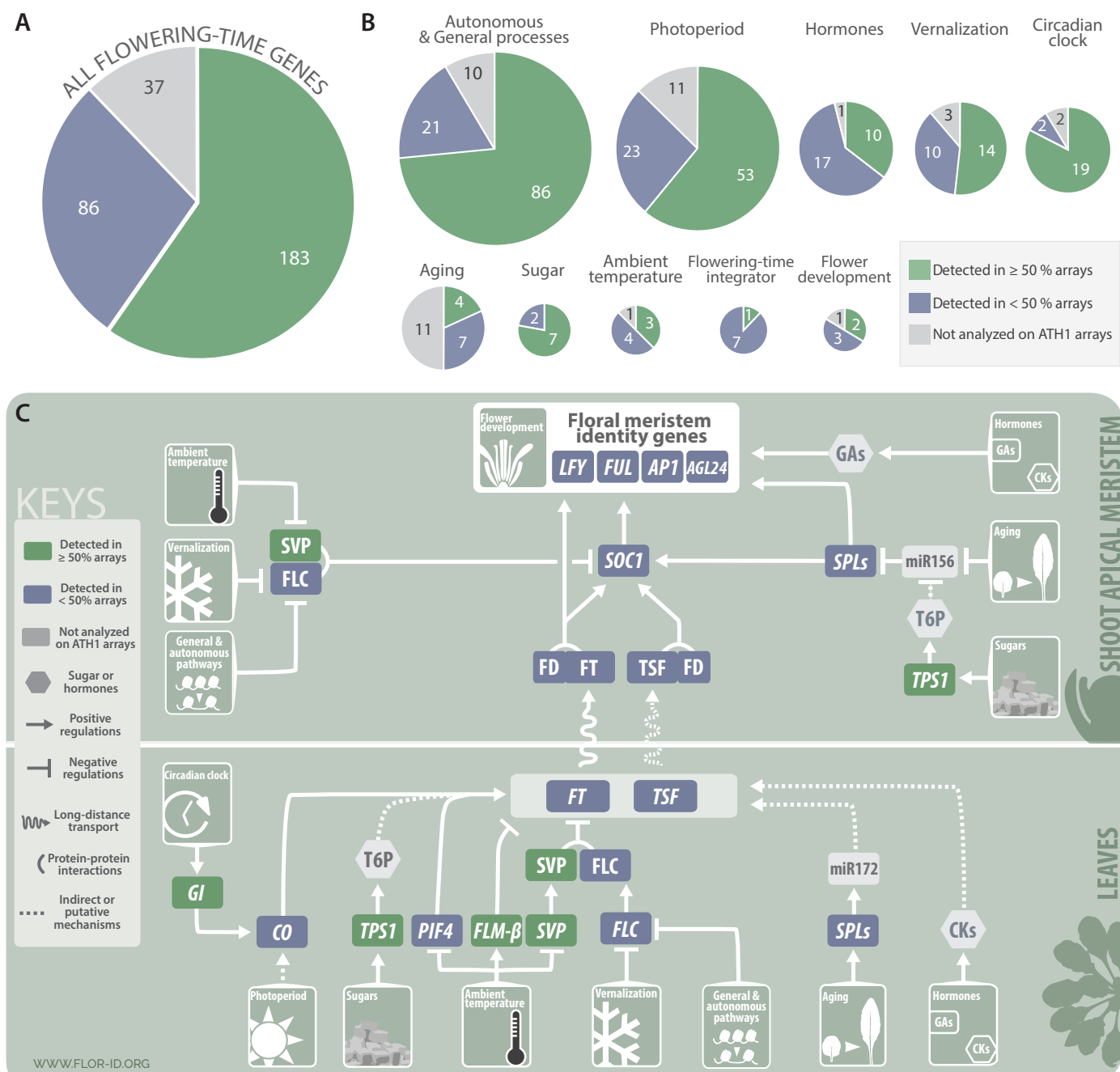


Figure 1. Flowering-time genes expressed in the roots of *Arabidopsis thaliana*. Root-expressed genes were identified by a present/absent call on 1,673 root ATH1 arrays retrieved from ArrayExpress repository (<https://www.ebi.ac.uk/arrayexpress/>). Flowering-time genes were extracted from FLOR-ID.

A. All 306 flowering genes. **B.** Pie charts showing the same set of genes classified into flowering time pathways, circadian clock and flower development. Some genes are involved in more than one pathway. Pie chart area is proportional to gene number. **C.** The snapshot of flowering pathways was extracted and adapted from FLOR-ID. Genes highlighted in green boxes were detected in ≥ 50% of root arrays. Genes in blue boxes were detected in < 50 % arrays. Genes and compounds not analyzed in ATH1 arrays are in grey.

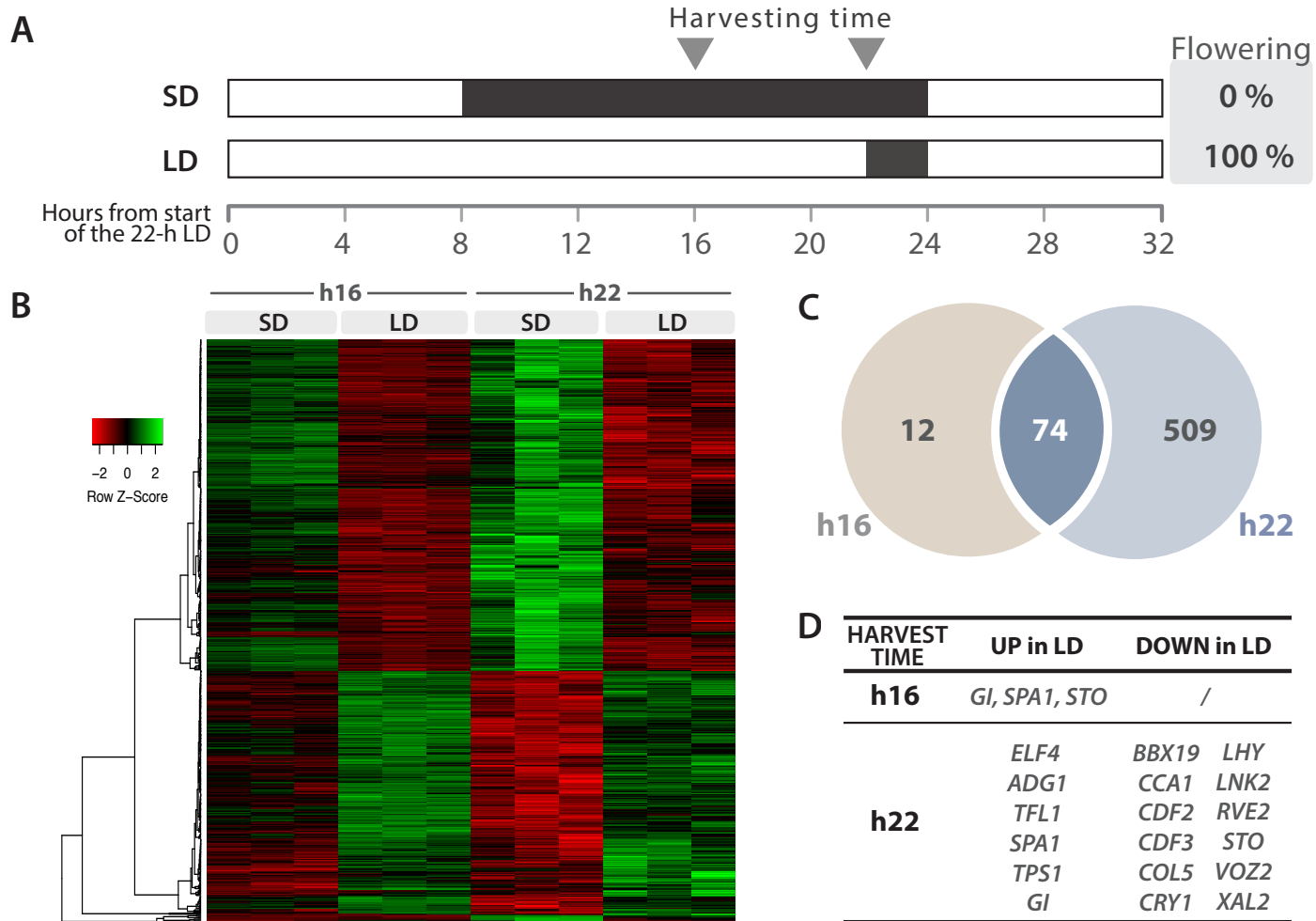
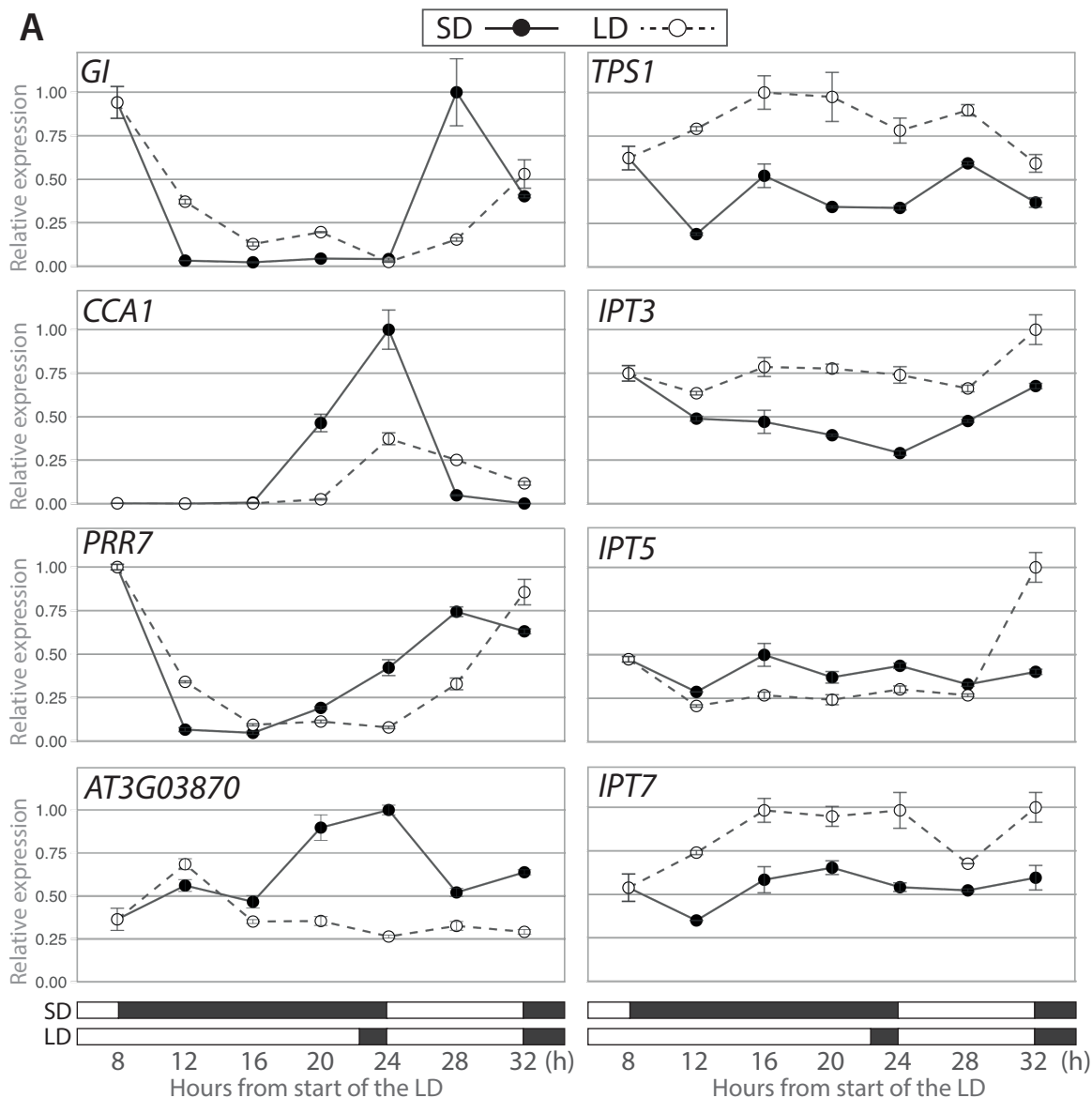


Figure 2. Root transcriptome changes during the induction of flowering by a single 22-h LD. A.

Experimental design. The proportions of plants having initiated flower buds two weeks after the experiment are shown on the right. **B.** Heatmap of the differentially expressed genes (adjusted p-value ≤ 0.01 ; fold-change ≥ 2) showing three independent biological replicates per condition. Low expression levels in red, high expression levels in green. Relative expression values are scaled per transcript (lines). **C.** Venn diagram of differentially expressed genes at both sampling time points. **D.** List of differentially expressed flowering-time genes.



B

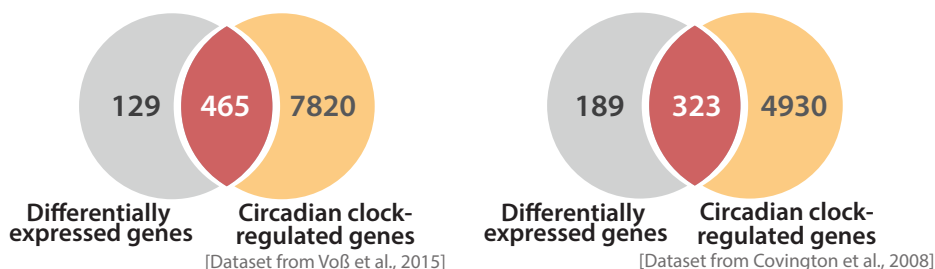


Figure 4. Temporal aspects of transcriptomic changes. **A.** Time-course analyses of candidate gene expression. Relative transcript levels were analysed by RT-qPCR during an 8-h SD (closed symbols) or a single 22-h LD (open symbols). Boxes in the bottom show light (white) and dark (black) periods. Data were normalized using *ACT2* and *UBQ10* genes. Error bars indicate the standard error of the mean for three experimental replicates. Data are from one representative experiment. **B.** Estimate of circadian clock-regulated differentially expressed genes. Venn diagrams showing the overlap between the differentially expressed genes identified in this study and the circadian clock-regulated genes expressed in lateral roots [left; Dataset from (Voss et al., 2015)] or in the shoot [right; Dataset from (Covington et al., 2008)].

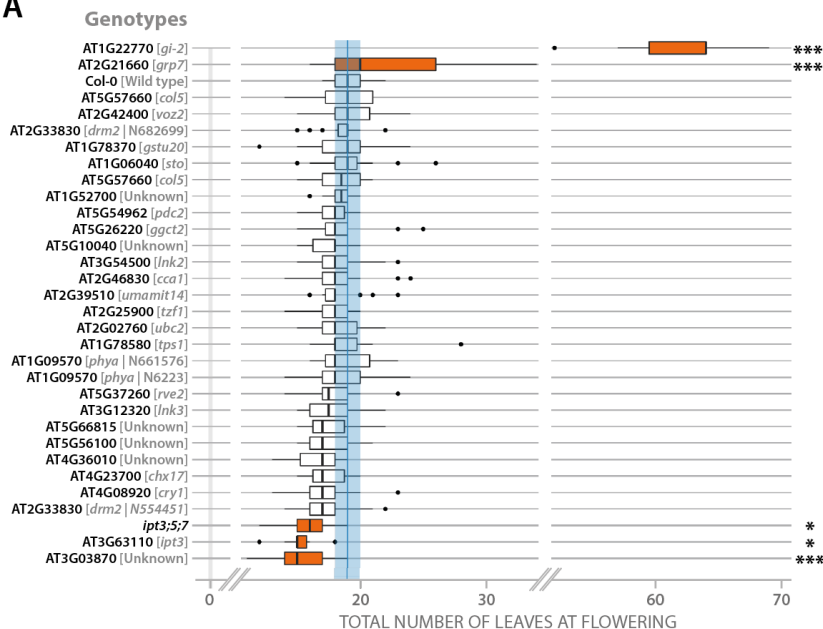
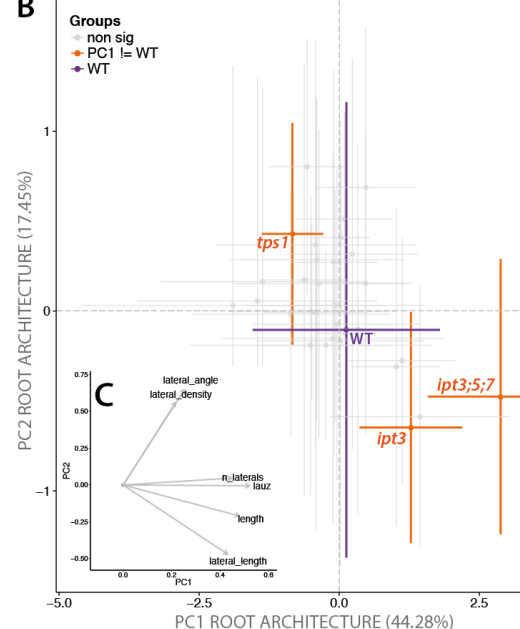
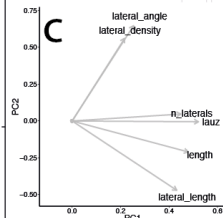
A**B****C**

Figure 5. Flowering-time and root architecture phenotypes of selected mutants in 16-h LD. A.

Total number of leaves below the first flower (n=15). * indicates a significant difference with WT Col-0 (Tukey's HSD test, $p < 0.05$). *** indicates a highly significant difference with WT (Tukey's HSD test, $p < 0.01$). WT is shown in blue. **B.** Plot of the first two components of the Principal Component Analysis performed on root system architecture features. **C.** Biplot of the two first components of the PCA.

Orange color indicates significant differences with the WT Col-0.